Space 2005
30 August - 1 September 2005, Long Beach, California

AIAA 2005-6653

Effect of Shielding Materials from SPEs on the Lunar and Mars Surface

Myung-Hee Y. Kim*
Wyle Laboratories, Houston, Texas, 77058

Xiaodong Hu†
USRA, Houston, Texas, 77058

and

Francis A. Cucinotta‡
NASA Johnson Space Center, Houston, Texas, 77058

Solar particle events (SPEs) are a health concern for astronauts who are involved in space missions outside the Earth's geomagnetic field. Here we examine the physical compositions and intensities of SPE exposures in sensitive astronaut tissues behind various shielding materials using the lunar and Mars surface environment during some historically large SPEs including the recent events of October 2003 and January 2005. The radiation risk at the sensitive tissues and the effective dose are assessed using the BRYNTRN code with the computerized anatomical man (CAM) model for the astronaut's body tissue. Additional calculations of the neutron flux are made using the PHITS code. The dose and dose rates of the most important events are calculated for the various shielding materials. Since the low-energy proton spectra are attenuated rapidly with shielding, the important factors for determining the exposure levels at sensitive tissue sites are the mass distribution of shielding materials and the astronaut's body. We show that chronic exposure to SPEs is the major risk while the risk of early effects is very small due to the reduction of dose-rates behind shielding (<1 cGy/h). Polyethylene, graphite carbon, the conventional vehicle material of aluminum, and the extra-terrestrial material of Martian regolith are considered in the current study. Results will guide the design of protection systems for astronauts in case of exposure to large solar particle events during future space missions.

Nomenclature

BFO = Blood Forming Organ
BRYNTRN = Baryon Transport
CAM = Computerized Anatomical Man model
CEV = Crew Exploration Vehicle
E = effective dose
EVA = Extra Vehicular Activity
GOES = Geostationary Operational Environmental Satellite
Gy-Eq = gray equivalent
J_0 = exponential spectral constant, protons/cm^2-s-sr
MCNPX = Monte Carlo radiation transport code
PHITS = Particle and Heavy-Ion Transport code System
P_0 = characteristic rigidity, MV

* Senior Scientist, Radiation Biophysics Laboratory, Wyle/HAC/37A, AIAA Member.
† Scientist, Division of Space Life Sciences, SK12, Non-AIAA Member.
‡ Project Chief Scientist/NASA Radiation Health Officer, Space Radiation Health Project, SK12, Non-AIAA Member.

rem = roentgen equivalent man, cSv
SPE = Solar Particle Event
Φ_{30} = integral fluence with energy above 30 MeV, protons/cm^2

I. Introduction

Solar particle events (SPEs) have been a concern for space missions outside the Earth's geomagnetic field since they were first verified from measurements taken at ground-level and using ion chambers on a high-altitude balloon[1,2] during the February 23, 1956 SPE. As a wide variety of monitoring techniques have been involved, concerns were further raised by a more intense intermediate energy event that occurred on November 12, 1960.[3,4] Since then very major SPEs were detected on Earth using a variety of measuring techniques during solar cycle 19, and since the 20th solar cycle, SPEs have been routinely detected by satellites.

Although the detection thresholds differed between the 19th and more recent cycles, a useful continuous database of 218 solar proton events has been generated for solar cycles 19-21.[5] To analyze SPEs over the past five solar cycles, the assembled list of MeV class SPEs in reference 5 was used for solar cycles 19-21, and satellite measurements from the synchronous orbiting GOES spacecraft[6] were used to calculate the proton fluences of the SPEs during solar cycles 22 and 23. The SPEs were then ranked according to the event-integrated proton fluences for energies above 30 MeV, and an association between the occurrence of large SPEs and solar activity was indicated. However, it also indicated that the major events were absent during the solar maximal months.

Astronaut's radiation exposure predictions are required for the mission planning and to implement health protection measures. Dose-rate is an important descriptor of both acute radiation effects and late cancer effects. For protons, large sparring occurs at dose-rates below about 20 cGy/h,, but the dose and dose-rate reduction factors (DDREFs) are only applicable below 5 cGy/h for cancer risk estimations.[7] To estimate dose and dose-rate distributions to astronauts from exposures to large SPEs, radiation transport properties of shielding materials and astronaut's body tissues were calculated by the BRYNTRN[8,9] code system. The typical shield configuration was assumed to be a spherical structure, and the astronaut body geometry was taken from the computerized anatomical man (CAM) model.[10] The temporal behaviors of organ dose rate and cumulative dose from two historically large events in November 1960 and August 1972, and from the recent large SPEs in October 2003 and January 2005 were analyzed behind various shielding thicknesses. The total spectra of these large SPEs and of February 1956 SPE were also considered to estimate shielding requirements for total exposure to large SPEs. Although alpha particles and heavier nuclei make variable contributions to SPEs, the current analyses were restricted to the proton components of SPEs because measurements generally show a significant heavy ion flux for particles with energies less than 20 MeV per nucleon and a homogeneous database of measurements is not available for the past five solar cycles. We also discuss additional calculations of the neutron flux using the Monte-Carlo transport code PHITS[11] to assess contributions from neutrons and protons that are produced from the interactions of high-energy SPE components with vehicle and surface material of regolith on the lunar and Mars surface.

II. Solar Particle Events: 1955-2005

The list of major SPEs and the proton fluences for solar cycles 19-21 (1955-1986) assembled by Shea and Smart[5] contain all the available flux and fluence data in the form of useful continuous database. From 1986 to the present (solar cycles 22 and 23), a SPE list and the GOES spacecraft measurements of the 5-min average integral proton flux[6] were obtained through direct access to NOAA's NGDC. For the completeness of the event-integrated fluences with energy above 30 MeV (Φ_{30}) of SPEs for the past five solar cycles, the SPE fluences for solar cycles 19-21 were taken from the reference 5, and those for the cycles of 22 and 23 were calculated using the extensive direct GOES satellite particle measurements of integral proton flux.[6] Table 1 lists the large SPEs for the past five solar cycles, where the omnidirectional proton fluence of Φ_{30} exceeds 10^9 protons/cm^2.

Table 1. Solar Proton Events during Solar Cycles 19-23 with $\Phi_{30} > 10^9$ protons/cm^2

Solar Cycle	Onset Time	Φ_{30}, protons/cm^2	Time to Peak Flux, hr	Comment
19	11/12/1960	9.00×10^9	14	(a), note 1
20	8/2/1972	5.00×10^9	69	(a)
22	10/19/1989 13:05	4.23×10^9	26.9	(b)
23	7/14/2000 10:45	3.74×10^9	25.8	(b)
23	10/26/2003 18:25	3.25×10^9	4.2	(b), note 2
23	11/4/2001 17:05	2.92×10^9	33.2	(b)

19	7/10/1959	2.30 x 10^9	note 3	(a)
23	11/8/2000 23:50	2.27 x 10^9	16.1	(b)
22	3/23/1991 8:20	1.74 x 10^9	19.5	(b)
22	8/12/1989 16:00	1.51 x 10^9	15.2	(b)
22	9/29/1989 12:05	1.35 x 10^9	14.1	(b)
23	1/16/2005 2:10	1.04 x 10^9	39.7	(b)
19	2/23/1956	1.00 x 10^9	note 4	(a)

(a) Φ_{30} for solar cycle 19-21: data taken from Shea and Smart[5]

Note 1: There are large differences in the estimate of fluence in November 1960 SPE. Data given by others[3, 4] are significantly smaller than the value given here. It is given as 1.3 x 10^9 protons/cm^2 by Freier and Webber.[4]

(b) Φ_{30} for solar cycle 22 and 23: calculated using corrected 5-min average proton flux of GOES measurements[6]

Note 2: Φ_{30} for the combined 3 major peaks occurred during 10/26-11/6/2003: 3.42 x 10^9 protons/cm^2

Note 3: Maximum peak in 1 day later on July 11, 1959; no exact time available[5]

Note 4: Maximum peak in the same day on February 23, 1956; no exact time available[5]

Using the list of 216 particle events recorded by NOAA's GOES satellite,[6] the event occurrences within 3 months period are plotted in Fig. 1-3 for solar cycles 21-23, respectively. Monthly mean sunspot numbers are included in these figures to show the association between SPE occurrence and solar activity. The distributions clearly show an increase in SPE occurrence with increasing solar activity; however, no recognizable pattern can be identified. Also, the occurrence times of large SPEs are marked with arrows in these figures: the criteria for these events having $\Phi_{30} > 10^9$ protons/cm^2 for cycles 22 and 23 (Fig. 2 and 3); and $\Phi_{30} > 10^8$ protons/cm^2 for the cycle 21 (Fig. 1), due to the absence of SPE having such large criteria of $\Phi_{30} > 10^9$ protons/cm^2 for this cycle. Large events have definitely occurred during solar active years, but have not occurred exactly during months of solar maximal activity. Moreover, they are more likely to occur in the ascending or declining phases of the solar cycle.[12] This sporadic behavior of SPE occurrence is a major operational problem in planning for Moon and Mars missions. However, historical large SPE environments are examined as one of probabilistic approaches for the protection and planning, and the examination can guide the design of protection systems for astronauts in case of exposure to large SPEs during future deep space missions.

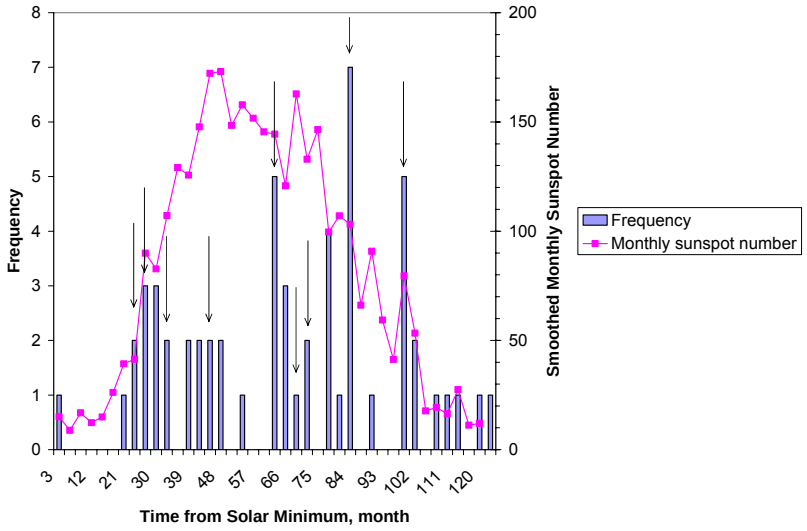

Figure 1. Frequency of SPE occurrence in three-month periods for solar cycle 21. The arrow indicates the occurrence time of SPE with $\Phi_{30} > 10^8$ protons/cm^2. From left: Feb 1978, Apr 1978, Sept 1978, Sept 1979, Apr 1981, Oct 1981, Jan 1982, Dec 1982, and Apr 1984.

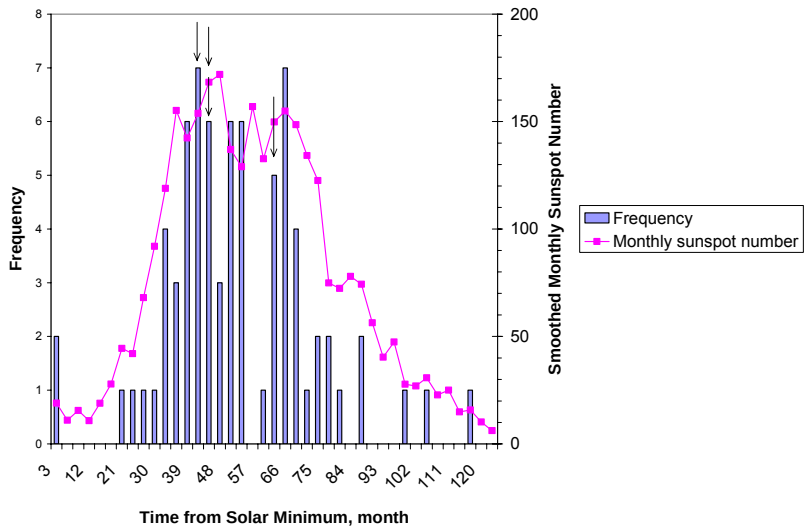

Figure 2. Frequency of SPE occurrence in three-month periods for solar cycle 22. The arrow indicates the occurrence time of large SPE with $\Phi_{30} > 10^9$ protons/cm^2. From left: Aug 1989, Sept 1989, Oct 1989, and Mar 1991.

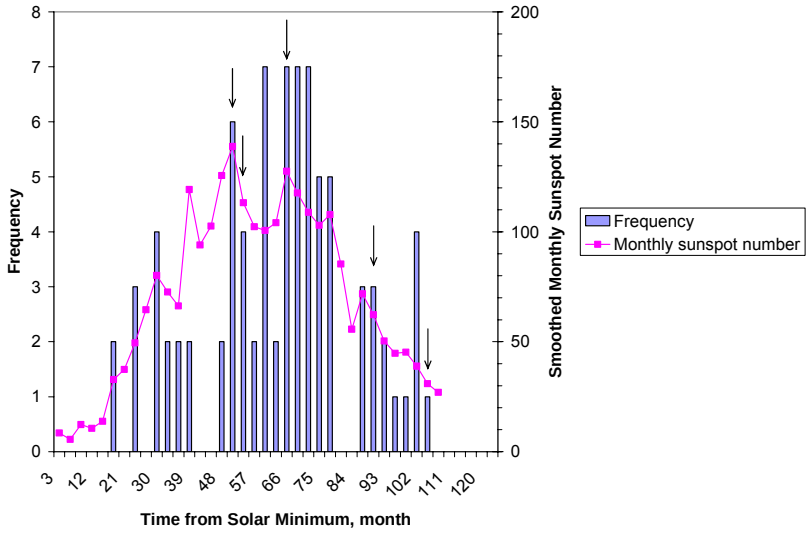

Figure 3. Frequency of SPE occurrence in three-month periods for solar cycle 23. The arrow indicates the occurrence time of large SPE with $\Phi_{30} > 10^9$ protons/cm^2. From left: Jul 2000, Nov 2000, Nov 2001, Oct 2003, and Jan 2005.

III. Radiation Transport at Sensitive Sites

The Baryon transport code system, BRYNTRN,[8, 9] was used to predict the propagation and interaction of the SPE nucleons through various media. This code includes the transport of light ions (n, p, ^{2}H, ^{3}H, ^{3}He, and α), and the local energy deposition for heavier target fragments, by solving the fundamental Boltzmann transport equation. Within the straight ahead and continuous slowing-down approximations, the transport equation is written as

$$\left[\frac{\partial}{\partial x} - \frac{\partial}{\partial E}\tilde{S}_j(E) + \sigma_j(E)\right]\phi_j(x,E) = \sum_{k\geq j}\int_E^\infty \sigma_{jk}(E,E')\phi_k(x,E')dE' \qquad (1)$$

where

$\phi_j(x,E)$	flux of ions of type j with atomic mass A_j having energy E (in units of MeV/amu) at spatial location x
σ_j	macroscopic total nuclear-absorption cross sections
$\widetilde{S}_j$	change in E per unit distance
σ_{jk}	differential nuclear-interaction cross sections

To evaluate the flux of particles of type j with energy E, the input database required consists of the stopping power, the macroscopic total nuclear cross sections, and the differential nuclear-interaction cross sections. The differential cross sections σ_{jk} describe the production of type j particles with energy E by type k particles of energies $E' > E$. These data are those compiled for the present BRYNTRN code system.[8, 9]

The absorbed dose D due to energy deposition at given location x by all particles is calculated according to

$$D(x) = \sum_j \int_0^\infty S_j(E)\phi_j(x,E)dE \tag{2}$$

For human exposure, the dose-equivalent is defined by the quality factor Q, which relates the biological damage incurred from any ionizing radiation to the damage produced by soft X-rays. In general, Q is a function of linear energy transfer (LET), which depends on both particle type and energy. For dose-equivalent calculations, the quality factors used are those defined by the International Commission on Radiological Protection in 1990 (ICRP 60).[13] The values of dose-equivalent H are computed at a given location x by all particles according to

$$H(x) = \sum_j \int_0^\infty Q_j(E)S_j(E)\phi_j(x,E)dE \tag{3}$$

Simple spacecraft geometry is chosen in which an astronaut is assumed to be at the center of a large spherical shell of uniform material with various shielding thicknesses. Inside a shield enclosure, three critical organs are considered: skin, ocular lens, and blood forming organ (BFO). Dose-equivalent at the critical site is calculated with the point particle fluxes of evenly spaced distribution of 512 rays over a 4 π solid angle that traverse water (the tissue equivalent material). The tissue thickness distribution surrounding a specific site is generated using the Computerized Anatomical Man (CAM) model,[10] which contains 2400 separate geometric tissue regions of several different elemental compositions and densities. The human body geometry is based on the 50 percentile United States Air Force male in the standing position. In addition to three critical sites, the effective dose is also considered for the radiation protection purpose, which is the representative quantity of stochastic effects for human body where the radiation quantities of individual organs or tissues are multiplied by their respective tissue weighting factors.[13, 14]

IV. Dose/Dose-Rate Distribution from SPE Exposure

Although the critical energy associated with the fluence depends on shielding, the critical fluences have been defined in an earlier study of shielding from SPE exposures in deep space.[15] Potentially debilitating events that are about one order of magnitude larger than those critical fluence levels were considered in the current study, i.e. two large events of November 12, 1960 SPE and August 2, 1972 SPE, and the recent large events of October 26, 2003 SPE and January 16, 2005 SPE; values of total fluences are listed in table 1.

A. The Hourly Distribution of SPE Fluence for Dose/Dose-Rate Distribution

Aside from the total fluence, the dose rate is an extremely important parameter for the biological response models. For low-LET radiation exposure such as protons, the biological damage is dependent on dose-rates.[7,16] Since SPEs have variable dose-rates that may extend above the so-called low dose-rate regime (5 cGy/h), dose-rate dependent factors over the time-course of SPEs could be important. To assess the temporal behavior of the large events, hourly exponential rigidity spectra were calculated with continuity of hourly-integrated proton fluences at 30 and 60 MeV, which were calculated using GOES data for October 2003 SPE and January 2005 SPE,[6] while those previously reported values[17] were used for August 1972 SPE. Fourteen exponential spectral determinations made by Freier and Webber[4] were used for the analysis of November 1960 SPE. The resultant proton differential energy spectra at each hour were transported through various thicknesses of spacecraft and body tissue materials to evaluate

the particle spectra at the sensitive sites using the BRYNTRN[8, 9] and the computerized anatomical man (CAM) model.[10]

Hourly-averaged proton fluxes of GOES data are shown in Fig. 4 during Oct 26 – Nov 6, 2003 SPEs, where three consecutive events occurred continuously for 12 days and the combined total fluence of Φ_{30} is stated in the note 2 of table 1. Time analyses for BFO dose rate and its cumulative dose equivalent behind various shielding thicknesses are shown in Fig. 5 and 6, respectively. Since the frequency of chromosomal aberrations is influenced significantly by dose rate, hourly BFO dose rates behind various spacecraft thicknesses are compared in Fig. 5. When 1 cGy/h is considered as the start of a transition from low to high dose rates, calculations indicate that the temporal behavior of dose rate at BFO is rather low for the October 2003 SPE except during the first major pulse. Furthermore, during high dose rate exposures protection can be easily achieved by adding a small amount of spacecraft material as shown in Fig. 5. The cumulative dose equivalent over the entire events of 12 days shown in Fig. 6 indicates the amount of exposure incurred from major peaks. During the peak times, the recommended exposure limit at BFO (25 cSv) is easily exceeded with the small amount of spacecraft material shown in this figure. The conventional amount of spacecraft material of 3-5 g/cm^2 shielding may provide adequate protection to avoid the short-term dose limit requirement on the Crew Exploration Vehicle (CEV) and other vehicles during this SPE as the current 30-day exposure limit is considered.

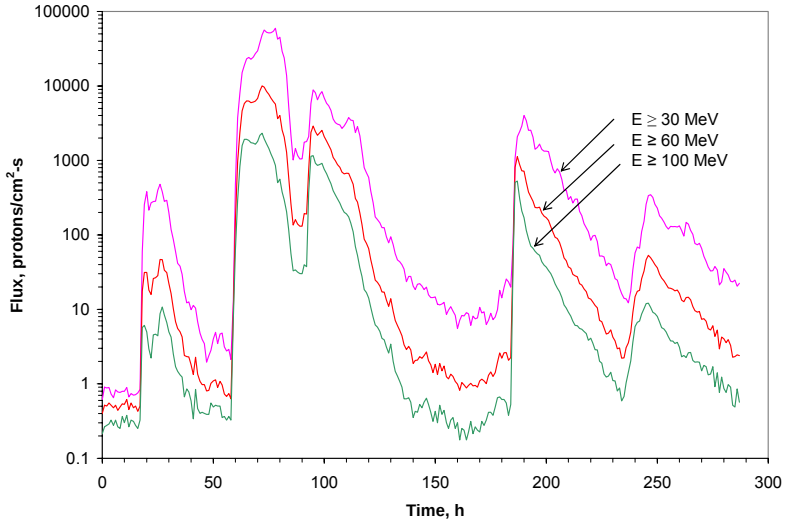

Figure 4. Hourly-averaged proton flux of GOES measurements during Oct 26-Nov 6, 2003 SPE.

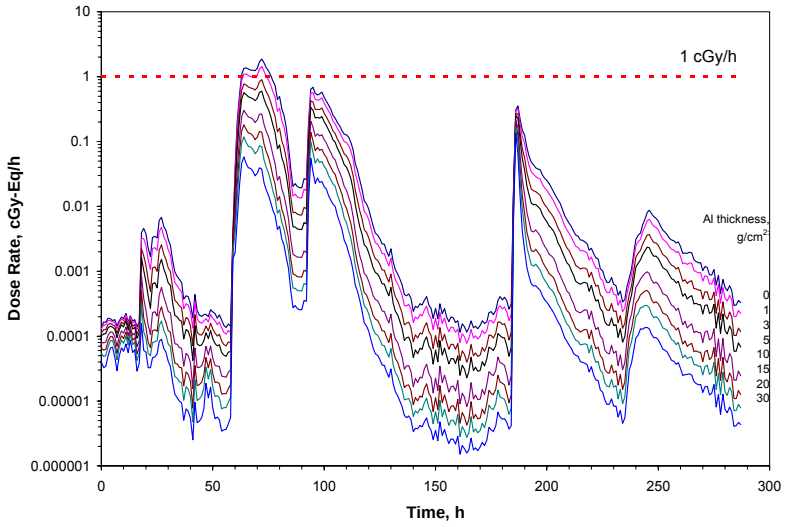

Figure 5. BFO dose rate behind various aluminum thicknesses during Oct 26-Nov 6, 2003 SPE.

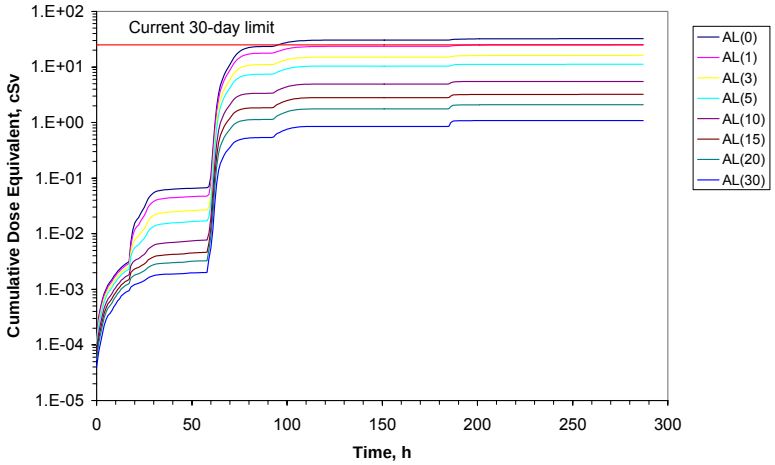

Figure 6. Cumulative BFO dose equivalent behind various aluminum thicknesses during Oct 26-Nov 6, 2003 SPE.

Dose rate effects were considered during the certain period of exposure times for the event of August 2-11, 1972.[17] The temporal behavior shown in Fig. 7 suggests significant biological damage would be incurred during the first major peak times. We note that biological effects are expected to increase significantly for dose rates above 5 cGy/h. For the major flux peak after the onset of the event, rather heavy shielding (up to 30 g/cm^2) provided would be insufficient to reduce the BFO dose rate below 1 cGy-Eq/h. The current recommended 30-day exposure limit at BFO is easily exceeded, and early effects from acute exposure may not be avoided when only conventional amount of spacecraft material is provided in order to protect BFO from this class of SPE as shown in Fig. 8. To avoid placing unrealistic mass on a space vehicle and at the same time to increase safety factors for astronauts, one shielding solution against SPE would be the selection of optimal vehicle/shielding materials, since it has been shown that materials with lower atomic mass constituents have better shielding effectiveness.[18, 19]

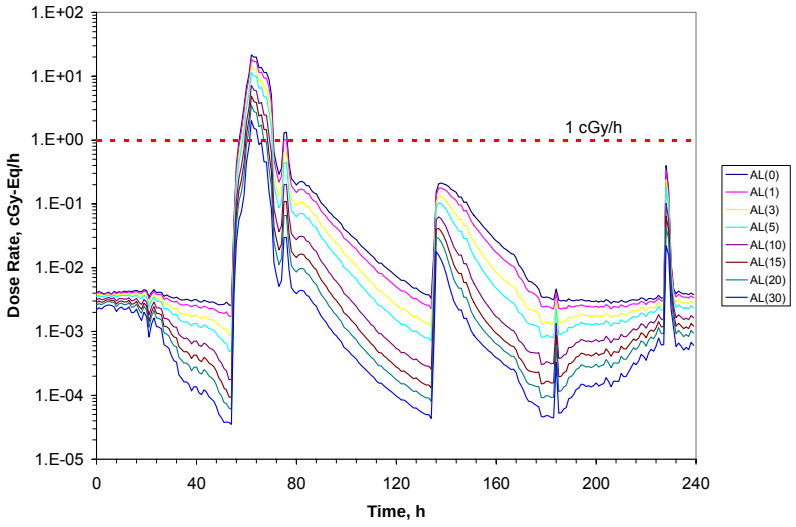

Figure 7. BFO dose rate behind various aluminum thicknesses during Aug 2-11, 1972 SPE.

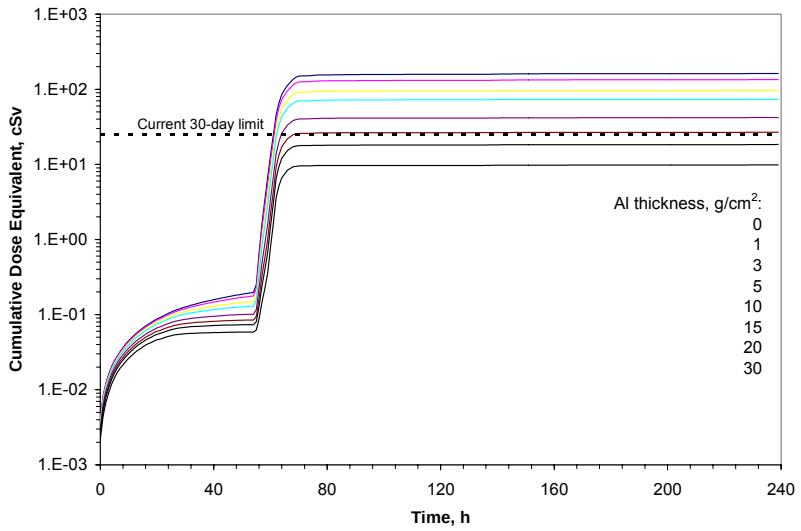

Figure 8. Cumulative BFO dose equivalent behind various aluminum thicknesses during Aug 2-11, 1972 SPE.

A wide variety of detection techniques have been used on balloons and satellites to measure the proton spectrum of all significant SPEs occurring in solar cycle 19.[3,4,20] There is rather detailed coverage for the event from November 12 to 16, 1960.[4] Fourteen limited spectral determinations of characteristic rigidity, P_0 (MV), and the constant, J_0 (protons/cm^2-s-sr), for the proton exponential spectra of November 12-16, 1960 SPE were derived using all available measurements by Freier and Webber[4] and listed here in table 2. The discrete time variations of proton flux and dose rate at each measurement were calculated with these spectral parameters shown in Fig. 9 and 10, respectively. In Fig. 10, the peak in dose rate within the several hours after optical flare is shown. During this peak period, about 15 g/cm^2 of spacecraft material of aluminum is required to reduce the BFO dose rate to below 1 cGy-Eq/h. Once again, the recommended current 30-day exposure limit at BFO is exceeded behind the conventional spacecraft shielding from this event as shown in Fig. 11.

Table 2. Exponential Spectral Determinations for Integral Fluences during November 12-16, 1960 Solar Particle Event.[4]

Date of SPE	Time of Optical Maximum	Time of Measurement	J_0, protons/cm^2 s sr	P_0, MV
Nov. 12, 1960[(a)]	13:29	11/12/60 19:30	1100	280
		11/12/60 20:00	1250	240
		11/13/60 02:00	3400	185
		11/13/60 08:00	3400	155
		11/13/60 13:05	3000	120
		11/13/60 18:30	2800	95
		11/13/60 20:00	2800	95
		11/13/60 22:30	1000	105
		11/14/60 05:00	1000	95
Nov. 15, 1960[(b)]	02:21	11/15/60 05:00	250	375
		11/15/60 10:30	320	240
		11/15/60 11:30	285	175
		11/15/60 12:30	285	175
		11/15/60 21:30	3300	120
		11/16/60 09:30	1000	100
		11/16/60 14:30	300	100
		11/16/60 17:30	300	100

[(a)] Event spectrum of Nov. 12, 1960 SPE = 3.68 x 10^9 $e^{-P(E)/158.6}$

[b] Event spectrum of Nov. 15, 1960 SPE = $2.47 \times 10^9 e^{-P(E)/136.6}$

[a] and [b] The combined event spectrum of November 12-16, 1960 SPE = $5.51 \times 10^9 e^{-P(E)/153.1}$

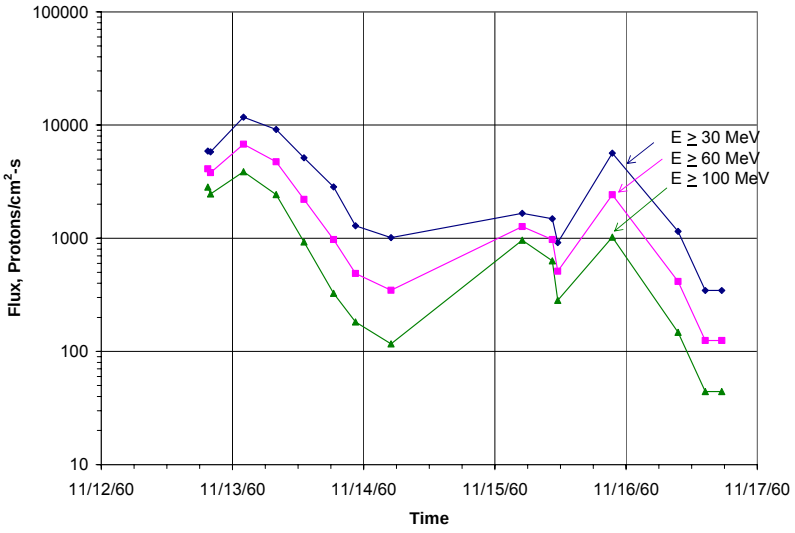

Figure 9. Proton flux at time of measurement during Nov 12-16, 1960 SPE.

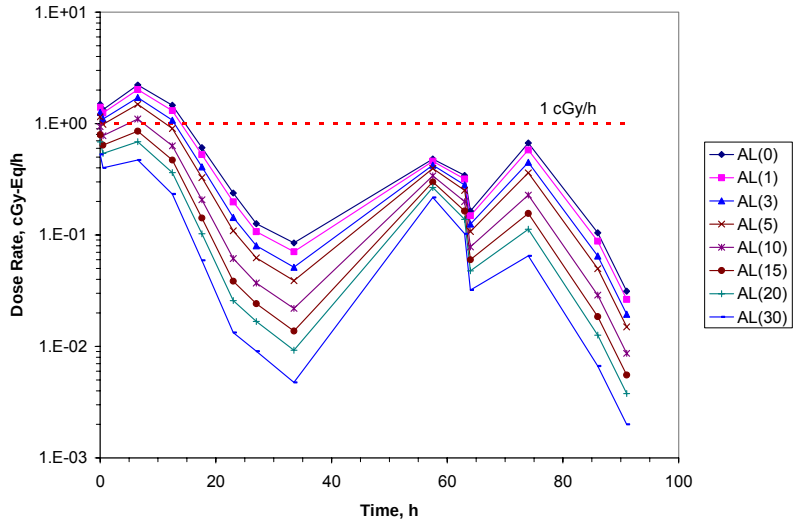

Figure 10. BFO dose rate behind various aluminum thicknesses during Nov 12-16, 1960 SPE.

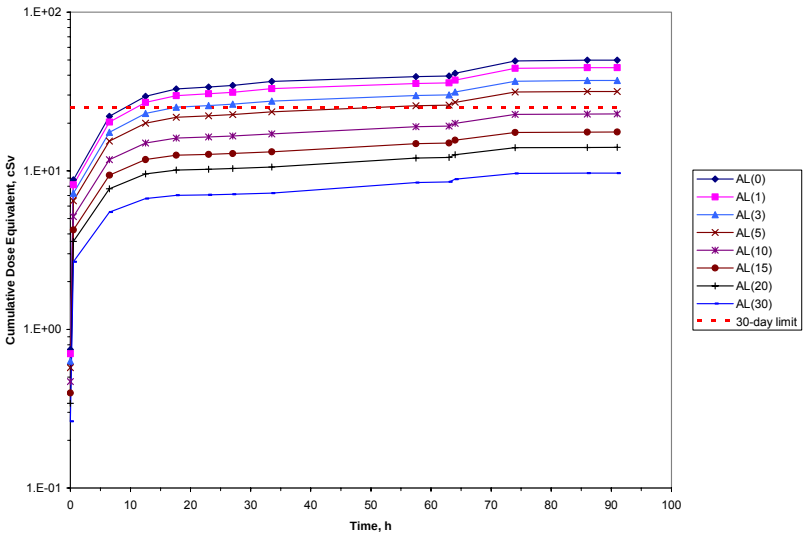

Figure 11. Cumulative BFO dose equivalent behind various aluminum thicknesses during Nov 12-16, 1960 SPE.

During the most recent event of January 16, 2005 SPE, there was a sudden increase in proton flux especially for particles with energies greater than 50 MeV, as shown in Fig. 12. Protons with energies greater than 100 MeV were increased by as much as four orders of magnitude after having declined from the major pulse. Although during this sharp commencement total fluence did not reach the value obtained at the major peak intensities, this sudden increase of high energy particles poses more threat than the major particle intensities as shown in Fig. 13. Dose rates at the second peak are increased by more than one order of magnitude compared to those of the first major pulse, and they are not lowered by adding more shielding in which minimal shielding effectiveness of aluminum has been shown. Although the cumulative dose from 7 days of exposure does not exceed the BFO exposure limit as shown in Fig. 14, the higher dose rates that result from the harder particle spectra in the sudden peak pose more radiation effect to human organ/tissue during this short period of time. It is noted that aluminum shielding is very efficient as adding more thicknesses during the major peak where large flux of particles are mostly low energies; while it is not efficient at all during the second sudden peak where high-energy components are increased rapidly to the SPE environment. With high-energy components in SPE, the material selection would be an efficient shielding strategy to reduce the particles' energy to below critical energy and also their fluences[18] as well as reducing vehicle mass.

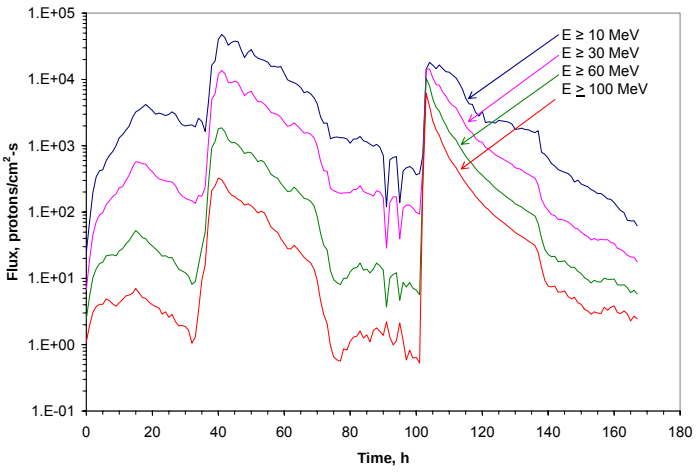

Figure 12. Hourly-averaged proton flux of GOES measurements during Jan 16-22, 2005 SPE.

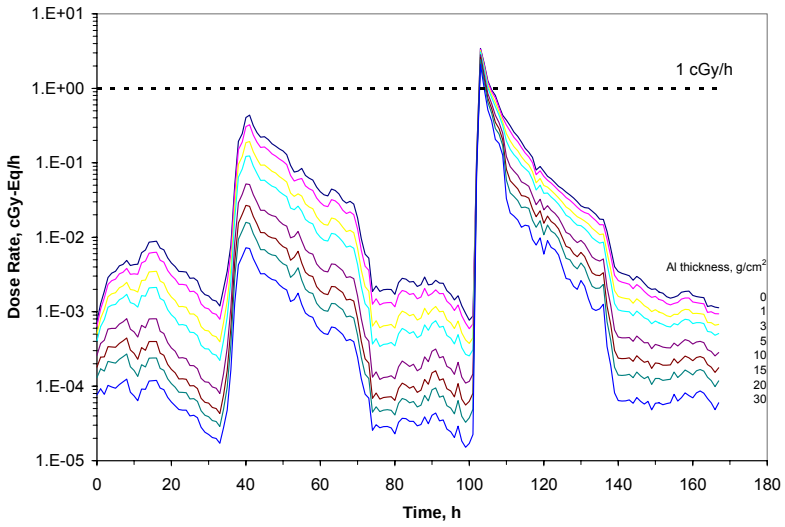

Figure 13. BFO dose rate behind various aluminum thicknesses during Jan 16-22, 2005 SPE.

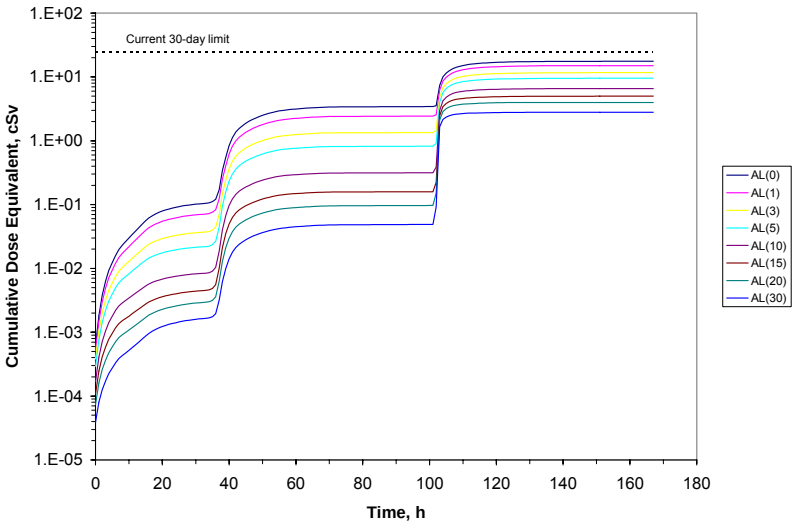

Figure 14. Cumulative BFO dose equivalent behind various aluminum thicknesses during Jan 16-22, 2005 SPE.

B. Total Exposure from the Large SPEs on Lunar and Mars Surface

An event of special interest occurred on February 23, 1956[15] where a striking feature was a large number of high-energy particles early in the event. However, there is still debate on the accuracy of spectral determinations for this event because only ground-based neutron monitors were available. Large uncertainties exist in the determination of spectra due to atmospheric propagation calculations that is required to unfold the spectra. Total dose equivalents are greater than 10 cSv (10 rem) at sensitive sites of skin, eye, BFO, and effective dose (E), even when various polyethylene shields are added to 20 g/cm^2 of spacecraft material in Fig. 15. However, these results should come with the caveat of significant uncertainties in the determination of the source spectra of protons.

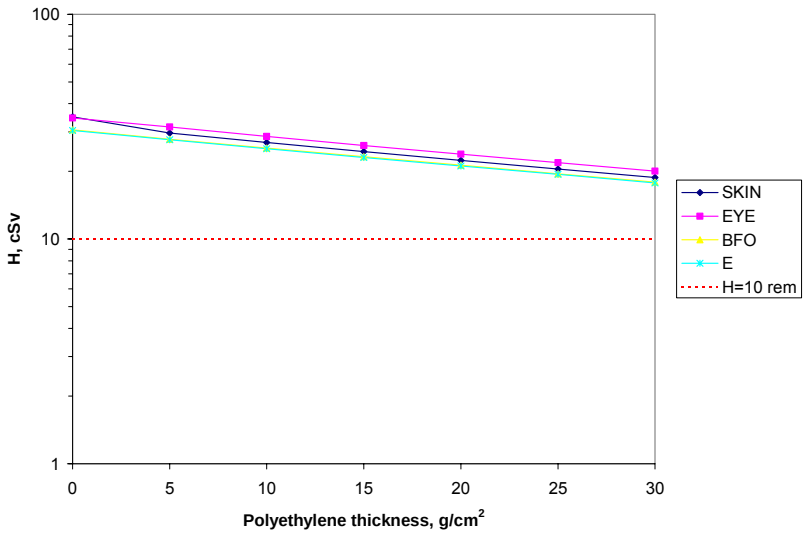

Figure 15. Dose equivalents at sensitive sites with various polyethylene shields added inside a 20 g/cm^2 of aluminum vehicle in free space from Feb 23, 1956 SPE exposure.

For other large historical events, total BFO dose can be lowered to below 10 cGy-Eq using a polyethylene storm shelter. To reduce overall exposure at BFO to below 10 cGy-Eq for August 1972 SPE, the required polyethylene shields are 11, 7, and 3 g/cm^2 inside 0, 5, and 10 g/cm^2 thicknesses of spacecraft material of aluminum, respectively. These are shown in Fig. 16 with exposures at skin, eye, and effective tissue.

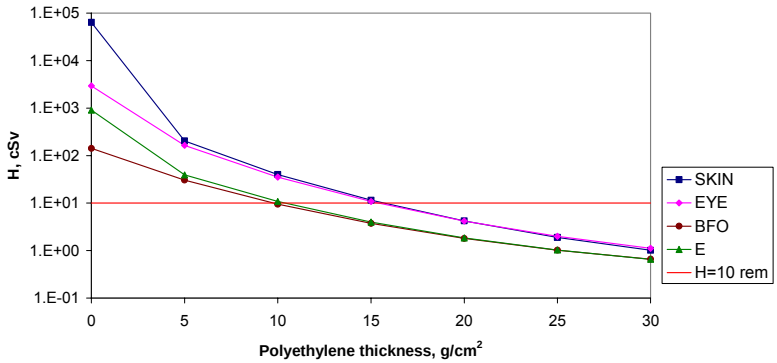

a) inside 0 g/cm^2 of aluminum

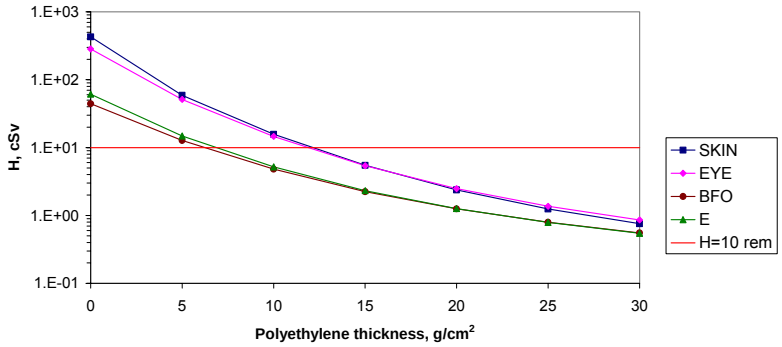

b) inside 5 g/cm^2 of aluminum

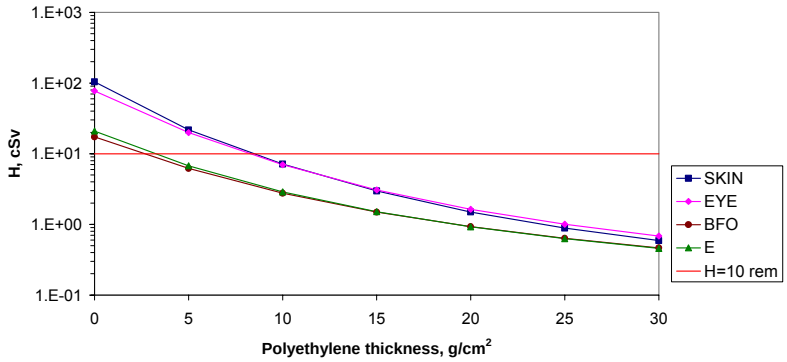

c) inside 10 g/cm^2 of aluminum

Figure 16. Dose equivalent at sensitive sites from Aug 1972 SPE with various polyethylene shields inside three aluminum vehicle thicknesses.

Calculations of the point dose equivalent and the effective dose, which is the tissue averaged organ dose equivalent, are compared for two shielding materials, graphite carbon and lunar/Martian regolith, from the August 1972 SPE in table 3. Also, included are the effective doses of aluminum, polyethylene, and liquid hydrogen to compare the shielding effectiveness. Exposure levels at effective tissue are reduced significantly by tissue shielding itself, since the low-energy proton spectra are attenuated rapidly as they traverse through the tissue materials. Hydrogen provides optimal protection and can be used in the form of fuel, water, or consumables although not in the primary structural material. Since graphite carbon, which is the backbone of carbon composites with significant hydrogen content and good structural properties, reduces the exposure level significantly when compared with aluminum, replacing aluminum vehicle with carbon composite for CEV and future spacecraft will reduce mass requirements at the same exposure level. Therefore, the effects of SPE are readily mitigated by the selection of shielding material and the tissue shielding, while the effects of GCR are not due to the contribution of target fragments in tissue and other uncertainties with high energy heavy ions.[21] A discussion of GCR is beyond the scope of this paper, however plays only a minor role for short term missions.

Table 3. Point dose equivalent and effective dose from August 1972 SPE.

	Point dose at tissue, cSv		Effective dose, cSv				
x, g/cm^2	Graphite Carbon	Regolith	Liquid Hydrogen	Polyethylene	Graphite Carbon	Regolith	Aluminum
0	151400	151400	354	354	354	354	354
5	590	756	11.9	43.7	50	56	66
10	128	173	1.9	13.4	16	19	24
20	15	22	0.2	3.15	3.5	4.0	6.3

SPE exposures on the lunar surface are reduced by approximately one-half by moon itself, and on the Mars surface by more than one-half due to the planet and the Mars atmosphere[22] of about 16 g/cm^2 vertical height of CO_2. Total exposures from the large SPEs are shown in table 4, which show that exposure levels are within the current limit for acute lethal response inside the conventional thickness (5 -10 g/cm^2) of spacecraft with various thicknesses of polyethylene storm shelter on lunar surface.

Table 4. Exposure from large SPE on lunar surface.

Al+PE thickness, g/cm^2		October 1989 SPE		August 1972 SPE		February 1956 SPE	
Al	PE	BFO, cGy-Eq	E, cSv	BFO, cGy-Eq	E, cSv	BFO, cGy-Eq	E, cSv
5	0	21.1	24.5	22.1	30.6	20.6	21.2
	5	9.7	10.0	6.4	7.4	17.6	17.5
	10	5.3	5.3	2.4	2.6	15.7	15.6
	20	2.1	2.0	0.6	0.6	13.0	12.9

	30	1.0	1.0	0.3	0.3	10.9	10.8
10	0	11.7	12.3	8.7	10.5	18.2	18.2
	5	6.2	6.2	3.1	3.4	16.1	16.0
	10	3.6	3.6	1.4	1.4	14.6	14.5
	20	1.5	1.5	0.5	0.5	12.1	12.1
	30	0.8	0.8	0.2	0.2	10.2	10.1

Based on the calculation of dose rate at BFO from August 1972 SPE shown in Fig. 7, the modest dose rates (< 5 cGy-Eq/h) are expected during the entire period of this event with realistic amounts of conventional spacecraft material. Further reduction of dose rates to less than 1 cGy/h can be obtained by utilizing optimized spacecraft and tissue shielding on lunar/Martian surface. Risks for acute radiation syndromes are possible only during the Extra Vehicular Activity (EVA), and a well designed EVA space suit, which utilizes the localized shielding concept, could provide sufficient protection to minimize this possibility. The prodromal response is the major acute risk from the SPE exposure in addition to the background exposure from the GCR that is not considered in the current study.

However, multiple SPEs (up to 7 events) have been occurred within 3-month period as shown in Fig. 1-3. Moreover, three major SPEs occurred within 3-month period in year 1989 as shown in Fig. 2: August 12, 1989 SPE, September 29, 1989 SPE, and October 19, 1989 SPE. The probabilities of acute radiation syndrome and chronic response are increased with increased mission duration, in which the much worse scenario is possible, such as multiple events with all of them to be large SPEs in the mission period. In that case, the mitigation of the effects of SPEs could be possible with employing other key strategies including accurate short-term SPE forecast and delayed mission planning for the protection of astronauts, in addition to optimization of shielding. Those worse cases will be carefully evaluated in the future.

C. Consideration of Secondary Neutron Contribution on Mars Surface

Secondary neutrons are produced by high-energy particles inside spacecraft and on lunar/Mars surface. While Martian atmosphere reduces charged particles on Martian surface, it also produces neutrons. Since the neutron albedo, which is not currently treated in BYRNTRN, might be a cause for the discrepancy for dose estimation on lunar and Mars surface,[23] additional calculations of the neutron flux produced by high-energy protons are made on Martian surface using PHITS[11] (Particle and Heavy-ion Transport code System).

PHITS (Particle and Heavy-ion Transport code System) developed at Japan Atomic Energy Research Institute (JAERI) is a multipurpose particle and heavy ion code. The code is made up with a combination of JAM (Jet AA Microscopic transportation model) and QMD (Quantum Molecular Dynamics) modules.[11] JAM is a hadronic cascade model. The trajectories of all hadrons as well as resonances including produced particles are followed explicitly as a function of space and time; the inelastic hadron-hadron collisions are described by resonance formation and decay at lower energies (below ~4GeV). Energy range of JAM extends from 100 MeV/u to about 100 GeV/u. QMD is a quantum extension of classic molecular-dynamics model. The QMD model is widely used to analyze various aspects of heavy ion reactions. JQMD is a QMD code developed at JAERI. JQMD includes SDM (Statistical Decay Model), and SDM is used for evaporation and fission decays of excited nuclei.[24] Energy range of this module is from 10 MeV/u to 3GeV. The data library used in the code is the same one that is used in MCNPX.[25] Then, PHITS gives same result as those of MCNPX in the data library driven energy region.

Fig. 17 shows the secondary neutron spectrum, which is back-scattered from Martian regolith, from 1 GeV proton beam after passing 16 g/cm^2 CO_2 Martian atmosphere. This spectrum presents the discrepancy, which might have been caused for dose estimation by BRYNTRN where the straight ahead and continuous slowing-down approximations are treated in BRYNTRN[8,9] at this point. This secondary neutron contribution will be implemented into BRYNTRN to improve the dose estimation. However, it appears that the dose contribution from these secondary would be minor, since the large productions are at low energies.

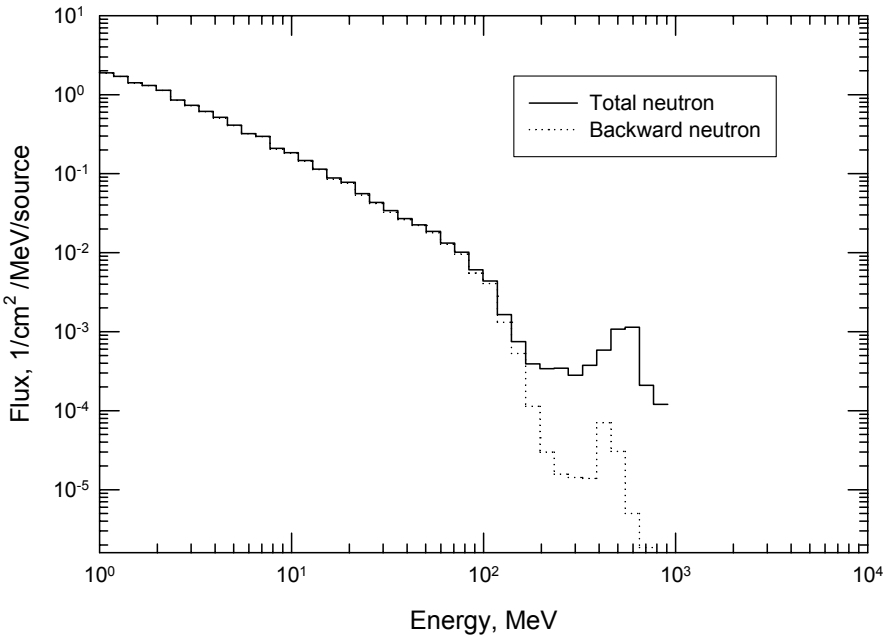

Figure 17. Energy spectra of neutron produced from 1 GeV proton on Martian surface in the cylinder region with radius of 0.5 m and height of 1 m.

V. Concluding Remarks

A complete list of SPEs for the past five solar cycles 19-23 was composed to find the association between SPE occurrence and solar activity. The distributions of SPEs clearly show an increase in SPE occurrence with increasing solar activity without recognizable pattern. From the inspection of historically large SPEs which are ranked according to the event-integrated proton fluences with energy above 30 MeV, the association between the occurrence of large SPEs and solar activity was indicated that the major events have been more likely occurred in the ascending or descending phases of solar cycle. This sporadic occurrence of SPEs and multiple occurrences of large SPEs in short period of time give problem to planning of space missions to moon and Mars.

Because dose rate dependent factors are expected to be important for biological responses, the detailed temporal behavior of historically large events is analyzed to guide the design of protection systems against exposure to large SPEs during future deep space missions. From the analysis, the doses received from most events are shown to be of low dose rates, because shielding mitigates most SPEs. For the event spectra of August 1972 SPE and November 1960 SPE, additional protection is required during certain periods of time at the major peak to avoid high dose rates. For January 2005 SPE, the fluxes of high-energy particles are increased rapidly without having the major particle intensities at low-energies. The resultant high dose rates from the harder spectra in this SPE require additional protection to avoid high exposure levels and biological responses during the rapid increase time of high-energy particles. Therefore, the accurate measurements of high-energy components of SPE are necessary which are often poorly measured.

For the reduction of overall exposure levels at BFO and other sensitive sites to less than 10 cSv from a large SPE, it can be achieved by adding effective shielding to various spacecraft thicknesses. In the case of having an event at high dose or dose rates in the future, astronauts require remaining in heavily shielded areas during peak dose rate times. Because dose rates can be reduced to less than 5 cGy/h inside polyethylene storm shelter (~ 10 g/cm^2), each of historically large SPEs can be characterized as low dose rates event except February 1956 SPE, which has a large number of high-energy particles. Shielding effectiveness has great impact on material selection especially from the exposure to SPEs with high-energy particles. Material with high radiation shielding effectiveness, such as polyethylene, offers about a factor of two less mass requirement for the same exposure level. It is also very efficient to stop the secondary neutrons produced inside spacecraft and on lunar/Mars surface.

Historically, multiple SPEs up to 7 events have been occurred during the short-term of three months. Moreover, couple of them is large SPEs in the same time period. The risk of early effects is usually very small from exposure

to an individual SPE. However, for a worse case, in which several large SPEs occur in a short mission period and each SPE is composed with a large number of high-energy particles, the risk of early effects will be increased significantly because shielding does not mitigate efficiently high-energy particles and it will be the added concern to the major risk of chronic exposure to SPEs. Therefore, a well shielded region with material having high radiation shielding effectiveness is required against SPE exposure to prevent a serious medical problem during lunar and Mars missions, especially in the series of large SPEs exposure during the mission period.

References

[1]Schafer, H. J., "Cosmic-ray Dosage during the Giant Solar Flare of February 23, 1956," *J. Aviation Med*., Vol. 28, 1957, pp. 387-396.

[2]Foelsche, T., "Protection against Solar Flare Protons," *Adv. Astronautical Sci*., Vol. 8, 1962, pp. 357-374.

[3]Biswas S., Fichtel, C. E., and Guss, D. E., "Study of the Hydrogen, Helium, and Heavy Nuclei in the November 12, 1960 Solar Cosmic-Ray Event," *Phys. Review*, Vol. 128, No. 6, 1962, pp. 2756-2771.

[4]Freier, P. S. and Webber, W. R., "Exponential Rigidity Spectrums for Solar-Flare Cosmic Rays," *J. Geophys. Res*., Vol. 68, No. 6, 1963, pp. 1605-1629.

[5]Shea, M. A. and Smart, D. F., "A Summary of Major Proton Events," *Solar Physics*, Vol. 127, 1990, pp. 297-320.

[6]National Geophysical Data Center (NGDC), GOES Space Environment Monitor, URL: http://goes.ngdc.noaa.gov/data/ [cited 17 June 2005].

[7]NCRP, "Radiation Protection Guidance for Activities in Low-Earth Orbit," Report 132, National Council on Radiation Protection and Measurements, Bethesda, MD, 2000.

[8]Wilson, J. W., Townsend, L. W., Nealy, J. E., Chun, S. Y., Hong, B. S., Buck, W. W., Lamkin, S. L., Ganapole, B. D., Kahn, F., and Cucinotta, F. A., "BRYNTRN: A Baryon transport model," NASA TP-2887, 1989.

[9]Cucinotta, F.A., Wilson, J.W., Badavi, F. F., "Extension to the BRYNTRN Code to Monoenergetic Light Ion Beams," NASA TP-3472, 1994.

[10]M. P. Billings and W. R. Yucker, "The Computerized Anatomical Man (CAM) Model," NASA CR-134043, 1973.

[11]Iwase, H., Niita, K., and Nakamura, T., "Development of General-Purpose Particle and Heavy Ion Transport Monte Carlo Code," *J. Nucl. Sci. and Technol*., Vol. 39, No. 11, 2002, pp. 1142-1151.

[12]Goswami, J. N., McGuire, R. E., Reedy, R. C., Lal, D., and Jha, R., "Solar Flare Protons and Alpha Particles during the Last Three Solar Cycles," *J. Geophys. Res.*, Vol. 93, No. A7, 1988, pp. 7195-7205.

[13]ICRP, "1990 Recommendations of the International Commission on Radiological Protection," ICRP Publication 60, Annals of the ICRP 21, International Commission on Radiological Protection, Elsevier Science, New York, 1991.

[14]NCRP, "Limitation of Exposure to Ionizing Radiation," Report 116, National Council on Radiation Protection and Measurements, Bethesda, MD, 1993.

[15]Wilson, J. W., Cucinotta, F. A., Shinn, J. L., Simonsen, L. C., Dubey, R. R., Jordan, W. R., Jones, T. D., Chang, C. K., and Kim, M. Y., "Shielding from Solar Particle Event Exposures in Deep Space," *Radiation Measurements*, Vol. 30, 1999, pp. 361-382.

[16]Simonsen, L. C., Cucinotta, F. A., Atwell, W. and Nealy, J. E., "Temporal Analysis of the October 1989 Proton Flare Using Computerized Anatomical Models," *Radiat. Res.*, Vol. 133, 1993, pp. 1-11.

[17]Unpublished records of a NASA workshop held several weeks after the event, correspondence dated October 24, 1972, from J. H. King at NASA Goddard Space Flight Center to A. C. Hardy at NASA Johnson Space Center.

[18]Wilson, J. W., Kim, M., Schimmerling, W., Badavi, F. F., Thibeault, S. A., Cucinotta, F. A., Shinn, J. L., and Kiefer, R., "Issues in Space Radiation Protection," *Health Physics*, Vol. 68, 1995, pp. 50-58.

[19]Cucinotta, F. A., Wilson, J. W., Williams, J. R., and Dicello, J. F., "Analysis of Mir-18 Results for Physical and Biological Dosimetry: Radiation Shielding Effectiveness in LEO," *Radiat. Meas.*, Vo. 32, 2000, pp. 181-191.

[20]Curtis, S. B., "Radiation Physics and Evaluation of Current Hazards," *Space Radiation Biology and Related Topics*, edited by C. A., Tobias and P. Todd, Academic Press, New York and London, 1974, pp. 21-99.

[21]Cucinotta, F. A., Kim, M. Y., and Ren, L., "Managing Lunar and Mars Mission Radiation Risks Part 1: Cancer Risks, Uncertainties and Shielding Effectiveness," NASA TP (in press)

[22]Simonsen, L. C., Nealy, J. E., Townsend, L. W., and Wilson, J. W., "Radiation Exposure for Manned Mars Surface Missions," NASA TP-2979, 1990.

[23]Shinn, J. L., Wilson, J. W., Lone, M. A., Wong, P. Y., and Costen, R. C., "Preliminary Estimates of Nucleon Fluxes in a Water Target Exposed to Solar-Flare Protons: BRYNTRN Versus Monte Carlo Code," NASA TM-4565, 1994.

[24]Niita, K., Chiba, S., Maruyama, T., Takada, H., Fukahori, T., Nakahara, Y., and Iwamoto, A., "Analysis of the (N,xN') Reactions by Quantum Molecular Dynamics plus Statistical Decay Model," *Phys. Rev*., Vol. C52, 1995, pp. 2620-2635.

[25]Hendricks, J. S. and the MCNPX Team, "MCNPX, Version 2.5.b," Los Alamos National Laboratory Report LA-UR-02-7086, 2002.